



Mitochondria-targeted fluorescent probe for rapid detection of thiols and its application in bioimaging

Yuedong Zhu, Haiting Pan, Yanyan Song, Chao Jing, Jia-An Gan, Junji Zhang*

Key Laboratory for Advanced Materials and Joint International Research Laboratory of Precision Chemistry and Molecular Engineering, Feringa Nobel Prize Scientist Joint Research Center, School of Chemistry and Molecular Engineering, Frontiers Center for Materio biology and Dynamic Chemistry, East China University of Science and Technology, Shanghai, 200237, PR China

ARTICLE INFO

Keywords:

Cyanine dyes
Biothiols
Mitochondria-targetable
Oxidative stress
PET

ABSTRACT

Biothiols are crucial reactive sulfur species in living cells, playing an essential role in maintaining the normal function of organisms. Effective detection of biothiols promotes the exploration of metabolic pathways and physiological functions of organisms. In this paper, a cyanine-based, mitochondria-targetable fluorescent probe, **Cy-DNBS**, was designed and synthesized. This probe uses a lipophilic cation unit as mitochondrial targeting site and DNBS group as the fluorescence quencher as well as the recognition site. The probe shows a distinct fluorescence emission at 604 nm upon rapid interaction with intracellular biothiols, owing to the removal of the 2,4-dinitrobenzene-sulfonyl (DNBS) group and the blockage of PET process. Moreover, the probe can not only image endogenous thiols, but also efficiently target mitochondria and evaluate thiol fluctuations under mitochondrial oxidative stress induced by H_2O_2 . Collectively, the new low cytotoxic probe can serve as a promising tool for monitoring cellular thiols and further exploring relevant disease processes.

1. Introduction

Mitochondria, which are considered as the cellular power packs, play vital roles in energy metabolism and apoptosis of cells, organs and tissues[1,2]. Moreover, mitochondria are the main source of intracellular reactive oxygen species (ROS) and related with various physiological processes[3,4]. However, excessive ROS can induce mitochondrial oxidative damage and eventually lead to numerous pathological conditions, including neurodegenerative disorders, cardiovascular diseases, diabetes, cancers and so on[5–8]. In order to protect cells from oxidative injury, mitochondria simultaneously possess a large number of free radical scavengers and mitochondria thiols, including homocysteine (Hcy), cysteine (Cys) and glutathione (GSH)[9–11], which are closely related to antioxidation processes in biological systems through the equilibrium of free thiols and oxidized disulfides forms[12–15], thus playing an essential role in complicated physiological and pathological processes[16–19]. The normal intracellular concentrations of Hcy, Cys and GSH are approximately 5–12 μ M, 30–200 μ M and 1–10 mM, respectively [20–23]. Large fluctuations in intracellular thiol concentrations will cause many diseases. For instance, low level of Cys has been reported to cause liver damage and lethargy[24,25]. Overexpression of Hcy results in neural tube defect and coronary heart disease[26]. GSH,

the most abundant intracellular biothiol, maintains redox homeostasis through protecting cells from injury caused by reactive oxygen species (ROS) and free radicals, which is quite significant for normal cell function[27,28]. Deviation from normal GSH concentration could lead to severe diseases as cancers. Many studies indicate that the above three mercaptan are related to each other and significantly decreased level of these thiols can cause mitochondrial damage and dysfunction[29–31]. In order to gain deeper understanding of the physiological mechanism and diagnosis of various related diseases, it is of essential importance to explore methods for real-time monitoring mitochondrial thiols fluctuations in living cells.

Fluorescence technique has aroused increasing interest due to the advantages of non-invasion, operational simplicity, high sensitivity/selectivity and fast response, and has witnessed great progress in the past decade[32]. Owing to the high reactivity of thiol groups, various fluorescent probes employing different mechanisms, such as Michael addition, disulfide exchange reaction, cyclization with aldehyde, nucleophilic substitution etc., have been developed for biothiol detection[33–38]. Maeda et al. [39] have reported that 2,4-dinitrobenzene-sulfonyl (DNBS) group has high sensitivity and responsiveness towards thiols, being useful to design thiol sensors. Inspired by this strategy, a new mitochondria-targeting probe **Cy-DNBS**, cyanine decorated with

* Corresponding author.

E-mail address: zhangjunji@ecust.edu.cn (J. Zhang).

<https://doi.org/10.1016/j.dyepig.2021.109376>

Received 15 March 2021; Received in revised form 3 April 2021; Accepted 3 April 2021

Available online 17 April 2021

0143-7208/© 2021 Elsevier Ltd. All rights reserved.

DNBS group, was designed and synthesized by our group for selective thiols detection and imaging *in vitro* and in living cell (Scheme 1). This probe uses a lipophilic cation unit as mitochondrial targeting site and DNBS group as the fluorescence quencher as well as the recognition site. Cy-DNBS shows no fluorescence in the absence of thiols due to the photo-induced electron transfer (PET) between fluorophore and DNBS group. Upon addition of thiols, distinct fluorescence emission at 604 nm can be detected owing to the removal of the DNBS group and the blockage of PET process. We investigated the spectral response of the probe in aqueous solution, and further in living cells. The results illustrated that the sensor displays high sensitivity and selectivity towards thiols and possesses excellent mitochondria-targeted ability.

2. Experiment

2.1. Materials and apparatus

All reagents and chemicals used for synthesis were purchased from commercial suppliers and used without further purification unless otherwise indicated. All oxygen or water sensitive reactions were performed under argon atmosphere using the standard Schlenk method. Mitotracker® Green FM and Hoechst 33342 were purchased from YEASEN Biological Company. HeLa, Du 145, PC-12 and HUVEV cells were purchased from ATCC (American Type Culture Collection).

The ^1H NMR and ^{13}C NMR spectra of compounds were recorded by Bruker AM-400 spectrometer, using tetramethylsilane (TMS) as an internal reference and CDCl_3 or $\text{DMSO-}d_6$ as solvent. MS spectra of compounds were measured on a Micromass LCTM (HREI-TOF) spectrometer. PBS buffers with different pH ranges were prepared using FiveEasy Plus pH meter. The absorption and emission spectra were recorded by Varian Cary 500 and Varian Cary Eclipse, respectively. Cell viability data were recorded by Synergy H4 Hybrid Reader (BioTek, USA). The cell confocal fluorescence imaging experiments were conducted on a Nikon (Japan) laser confocal scanning microscope.

2.2. Synthesis and characterization

Synthesis of compound 1. 2,3,3-Trimethyl-3H-indole (4.0 mL, 25 mmol) was dissolved in CH_3CN (15 mL). To the mixture was added CH_3I (4.0 mL, 60 mmol). Then the mixture was refluxed at 80°C overnight under argon atmosphere. After cooling to room temperature, the precipitate was filtered and washed with *n*-hexane and dried in vacuum to obtain compound 1 as a pale pink solid powder (6.68 g, yield 85.8%). ^1H NMR (400 MHz, $\text{DMSO-}d_6$) δ (ppm) 7.92 (dd, $J = 8.81$ Hz, 1H), 7.84 (m, $J = 8.57$ Hz, 1H), 7.63 (m, $J = 22.25$ Hz, 2H), 3.98 (s, 3H), 2.77 (s, 3H), 1.53 (s, 6H).

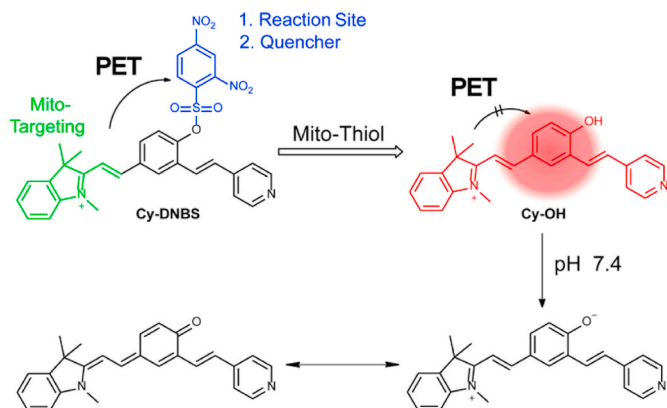
Synthesis of compound 2. To a 200 mL Schlenk tube, $\text{Pd}(\text{OAc})_2$ (0.60 g, 2.67 mmol), tri-*o*-tolylphosphane (1.64 g, 5.37 mmol) and 3-

bromo-4-hydroxybenzaldehyde (3.00 g, 14.92 mmol) were added. Then distilled toluene and triethylamine were injected under argon atmosphere after dehydration. After freezing and filtrating of oxygen, 4-vinylpyridine (2.0 mL, 18.81 mmol) was added. Then the mixture was refluxed at 100°C overnight and monitored by TLC. The reaction mixture was poured into CH_2Cl_2 after cooling to room temperature and filtered. The filtrate was washed with weak acid water and the aqueous layer was extracted with CH_2Cl_2 for three times. The combined organic layers were dried over anhydrous MgSO_4 and purified by column chromatography on silica gel with $\text{CH}_2\text{Cl}_2/\text{MeOH}$ (50:1, v/v) as eluent to get compound 2 as a pale yellow solid (1.20 g, yield 35.7%). ^1H NMR (400 MHz, $\text{DMSO-}d_6$) δ (ppm) 11.22 (s, 1H), 9.87 (s, 1H), 8.56 (d, $J = 5.90$ Hz, 2H), 8.21 (d, $J = 2.01$ Hz, 1H), 7.75 (dd, $J = 10.46$ Hz, 1H), 7.69 (d, $J = 16.57$ Hz, 1H), 7.57 (d, $J = 6.16$ Hz, 2H), 7.38 (d, $J = 16.57$ Hz, 1H), 7.06 (d, $J = 8.42$ Hz, 1H). ^{13}C NMR (101 MHz, $\text{DMSO-}d_6$) δ (ppm) 191.24, 161.21, 150.14, 144.45, 131.09, 129.95, 128.59, 127.08, 123.51, 120.82, 116.46. HRMS-ESI (m/z): Calcd. for $(\text{C}_{14}\text{H}_{11}\text{NO}_2)$: 226.0863 ($M + \text{H}^+$), found 226.0862.

Synthesis of compound 3. To a 100 mL three-neck round-bottom flask, compound 2 (0.30 g, 1.33 mmol) in dry CH_2Cl_2 and NEt_3 was added. The mixture was stirred at 0°C in ice-water bath for 60 min and 2,4-dinitrobenzenesulfonyl chloride (0.53 g, 2.00 mmol) in CH_2Cl_2 was added dropwise. Then the mixture was stirred at room temperature and monitored by TLC. After completion, the resulting mixture was filtered and the filter cake was dried in vacuum to get compound 3 as a pale yellow solid (0.54 g, yield 89.1%). ^1H NMR (400 MHz, $\text{DMSO-}d_6$) δ (ppm) 10.08 (s, 1H), 8.95 (d, $J = 2.25$ Hz, 1H), 8.55 (d, $J = 5.96$ Hz, 2H), 8.47 (dd, $J = 11.03$ Hz, 1H), 8.42 (d, $J = 1.77$ Hz, 1H), 8.25 (d, $J = 8.54$ Hz, 1H), 8.00 (dd, $J = 10.39$ Hz, 1H), 7.60 (d, $J = 8.33$ Hz, 1H), 7.35 (dd, $J = 18.15$ Hz, 3H), 7.23 (d, $J = 16.45$ Hz, 1H). ^{13}C NMR (101 MHz, $\text{DMSO-}d_6$) δ (ppm) 191.19, 151.22, 150.25, 149.59, 147.93, 142.69, 135.78, 133.54, 131.01, 130.79, 130.56, 129.12, 127.43, 124.76, 123.74, 120.76. HRMS-ESI (m/z): Calcd. for $(\text{C}_{20}\text{H}_{13}\text{N}_3\text{O}_8\text{S})$: 454.0351 ($M - \text{H}^-$), found 454.0356.

Synthesis of compound Cy-DNBS. To a 50 mL Schlenk tube, compound 1 (0.20 g, 0.66 mmol), compound 3 (0.30 g, 0.66 mmol) and NaOAc (0.05 g, 0.66 mmol) were added and acetic anhydride (10 mL) was injected under argon atmosphere after dehydration. Then the mixture was refluxed at 80°C for 6 h. After cooling to room temperature, the reactive mixture was suspended in diethyl ether and filtered to yield Cy-DNBS as a brown solid (0.20 g, yield 42.2%). ^1H NMR (400 MHz, $\text{DMSO-}d_6$) δ (ppm) 8.94 (d, $J = 2.26$ Hz, 1H), 8.77 (d, $J = 6.34$ Hz, 2H), 8.74 (d, $J = 1.39$ Hz, 1H), 8.50 (d, $J = 2.41$ Hz, 1H), 8.47 (m, $J = 10.53$ Hz, 1H), 8.43 (dd, $J = 10.62$ Hz, 1H), 8.26 (d, $J = 8.72$ Hz, 1H), 7.98 (dd, $J = 9.06$ Hz, 1H), 7.94 (dd, $J = 8.73$ Hz, 1H), 7.83 (d, $J = 16.52$ Hz, 1H), 7.77 (d, $J = 6.36$ Hz, 2H), 7.68 (dd, $J = 8.84$ Hz, 2H), 7.64 (d, $J = 8.81$ Hz, 1H), 7.56 (d, $J = 16.30$ Hz, 1H), 7.37 (d, $J = 16.38$ Hz, 1H), 4.25 (s, 3H), 1.85 (s, 6H). ^{13}C NMR (101 MHz, $\text{DMSO-}d_6$) δ (ppm) 181.71, 151.28, 150.00, 148.55, 147.97, 145.94, 143.79, 141.80, 134.77, 133.65, 131.77, 130.47, 130.37, 129.85, 129.42, 129.05, 127.45, 124.77, 122.96, 122.24, 120.69, 115.60, 115.27, 52.48, 25.04, 21.02. HRMS-ESI (m/z): Calcd. for $(\text{C}_{32}\text{H}_{27}\text{N}_4\text{O}_7\text{S}^+)$: 611.1595 (M^+), found 611.1641.

Synthesis of compound Cy-OH. To a 50 mL Schlenk tube, compound 1 (0.15 g, 0.49 mmol) and compound 2 (0.10 g, 0.44 mmol) were added. After dehydration, EtOH (3 mL) and pyridine (0.4 mL) were injected successively under argon atmosphere. Then the mixture was refluxed at 80°C for 4 h. The reactive mixture was filtered after cooling to room temperature. The filter cake was washed with EtOH and dried in vacuum to yield Cy-OH as a rufous solid (74 mg, yield 32.8%). ^1H NMR (400 MHz, $\text{DMSO-}d_6$) δ (ppm) 11.44 (s, 1H), 8.59 (d, $J = 6.07$ Hz, 2H), 8.54 (d, $J = 1.81$ Hz, 1H), 8.41 (d, $J = 16.29$ Hz, 1H), 8.14 (dd, $J = 10.58$ Hz, 1H), 7.87 (m, $J = 11.55$ Hz, 2H), 7.70 (d, $J = 16.46$ Hz, 1H), 7.65-7.53 (m, 5H), 7.41 (d, $J = 16.40$ Hz, 1H), 7.09 (d, $J = 8.52$ Hz, 1H), 4.13 (s, 3H), 1.81 (s, 6H). ^{13}C NMR (101 MHz, $\text{DMSO-}d_6$) δ (ppm) 181.39, 161.22, 153.46, 150.15, 144.56, 143.23, 141.87, 132.53,



Scheme 1. Proposed sensing mechanism of Cy-DNBS to thiols.

131.31, 128.85, 128.78, 127.10, 126.18, 124.18, 122.79, 120.83, 117.05, 114.68, 109.77, 51.79, 34.57, 25.66. HRMS-ESI (m/z): Calcd. for ($C_{26}H_{25}N_2O^+$): 381.1961 (M)⁺, found 381.1959.

2.3. Limit of detection (LOD)

The limit of detection was calculated according to the fluorescence titration curve of probe **Cy-DNBS** in the presence of thiols. We measured the fluorescence intensity of **Cy-DNBS** for 10 times and then calculated the standard deviation of blank measurement. The limit of detection was calculated according to the following equation:

$$LOD = 3\sigma/k$$

where σ is the standard deviation of the blank measurement, k is the slope between the fluorescence intensity versus thiol concentrations.

2.4. Cell culture and fluorescence imaging

HeLa, PC-12 and HUVEC cells were cultured at 37 °C in DMEM (Gibco, Gland Island, NY, USA) while Du 145 cells were cultured at 37 °C in MEM (Gibco, Gland Island, NY, USA) supplemented with 10% fetal bovine serum (Gibco, Gland Island, NY, USA) and 1% penicillin-streptomycin in humidified environment of 5% CO₂.

Cytotoxicity was estimated by cell counting kit-8 (CCK-8) assay. Firstly, cells were seeded into 96-well plates at 1×10^4 /well and cultured at 37 °C in humidified environment of 5% CO₂ for 24 h. Secondly, different concentrations of probe (0, 1, 2.5, 5, 10, 20 μ M) were added to wells and cells were incubated for 12 h. Finally, CCK-8 was added to each well and incubated for 30 min. The OD450 (absorbance value) was recorded by Synergy H4 Hybrid reader (BioTek, USA).

Cells were seeded on confocal cuvette and allowed to adhere for 12 h. For colocalization experiment, cells were incubated with 5 μ M **Cy-DNBS** for 30 min. After washed with PBS (2 mL \times 2 times), cells were incubated with 250 nM MitoTracker® Green FM for 30 min (or 5 μ g/mL Hoechst 33342 for 10 min). Finally, cell imaging was carried by laser confocal scanning microscope (Nikon, Japan) after washed with PBS (2 mL \times 2 times). For endogenous thiol imaging experiment and H₂O₂ induce oxidative stress experiment, cells were divided into three groups. The first group was untreated. The second group was incubated with 5 μ M **Cy-DNBS** for 30 min. The last group was pre-treated with 500 μ M N-phenylmaleimide (or 1 mM H₂O₂) for 30 min and then incubated with 5 μ M **Cy-DNBS** for 30 min after washed with PBS (2 mL \times 2 times). All group were washed with PBS (2 mL \times 2 times) before imaging. Emission

from MitoTracker® Green FM channel, λ_{ex} = 488 nm, λ_{em} = 500–550 nm; emission from Hoechst 33342 channel, λ_{ex} = 404 nm, λ_{em} = 425–475 nm; emission from **Cy-DNBS** channel, λ_{ex} = 561 nm, λ_{em} = 570–620 nm.

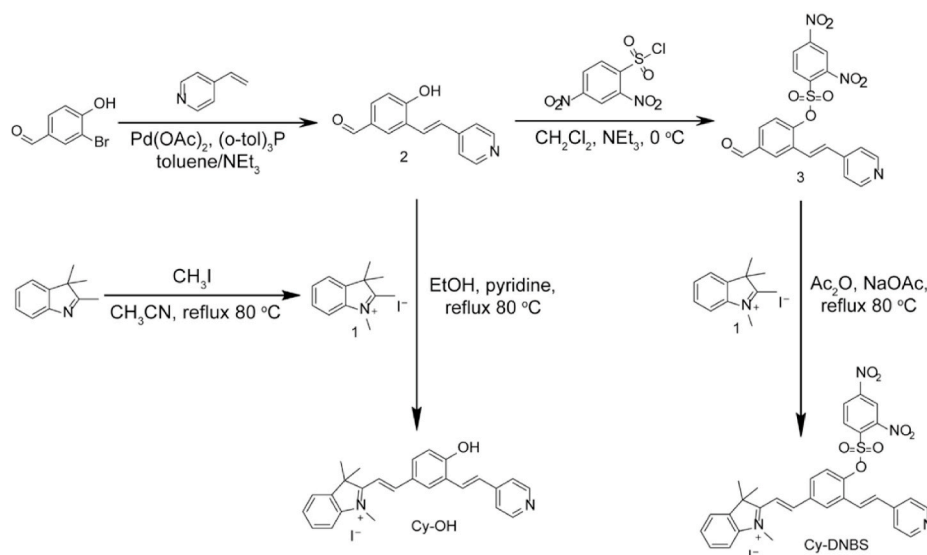
3. Results and discussion

3.1. Design and synthesis

Cyanine derivative was selected as the fluorophore due to its excellent photophysical properties and the positively charged moiety of indole ammonium cation for mitochondria targeting. 2,4-dinitrobenzenesulfonyl (DNBS) group was modified at the hydroxyl site of the fluorophore as both a thiol responsive group and quencher. **Cy-DNBS** probe was synthesized through a three-step synthesis shown in Scheme 2. Structure of all new compounds were characterized by ¹H NMR, ¹³C NMR and HRMS (see SI for details). After recognizing thiols, distinct fluorescence emission at 604 nm can be detected due to the removal of the DNBS group and blockage of PET process. ESI-MS was carried out to verify the reaction mechanism. As demonstrated in Fig. S1, **Cy-DNBS** shows a characteristic peak of m/z 611.1594 ($[M]^+$ calcd 611.1595). The new peak at m/z 381.1955 assigned to cleavable product **Cy-OH** ($[M]^+$ calcd 381.1961) was observed after adding GSH.

3.2. Spectral responses of Cy-DNBS toward thiols

With the probe in hand, we first investigated the optical response of **Cy-DNBS** toward thiols in phosphate buffered saline (PBS, 0.01 mM, pH 7.4 containing 10% DMSO). As shown in Fig. 1A, free **Cy-DNBS** exhibited two absorption maxima around 300 nm and 380 nm belonging to the DNBS and cyanine moieties, respectively. The absorption band at 380 nm disappeared with the addition of thiols, accompanied with the appearance of a new absorption band at 545 nm. **Cy-DNBS** alone displayed extremely minimized fluorescence and an obvious fluorescence emission signal at 604 nm appeared after interacting with thiols, which became stronger with the increasing concentration of thiols (Fig. 1B). The fluorescence intensity at 604 nm was linearly proportional to the GSH concentration in the range of 0–4 μ M with a limit of detection (LOD) of 1.38×10^{-7} M (Fig. 1C). Under the same conditions, **Cy-DNBS** exhibited similar fluorescence responses to Cys and Hcy with LODs of 1.34×10^{-7} M and 2.29×10^{-7} M, respectively (Fig. S2–S3). These results illustrated that **Cy-DNBS** shows excellent sensitivity towards thiols.



Scheme 2. The synthetic route of **Cy-DNBS** and **Cy-OH**.

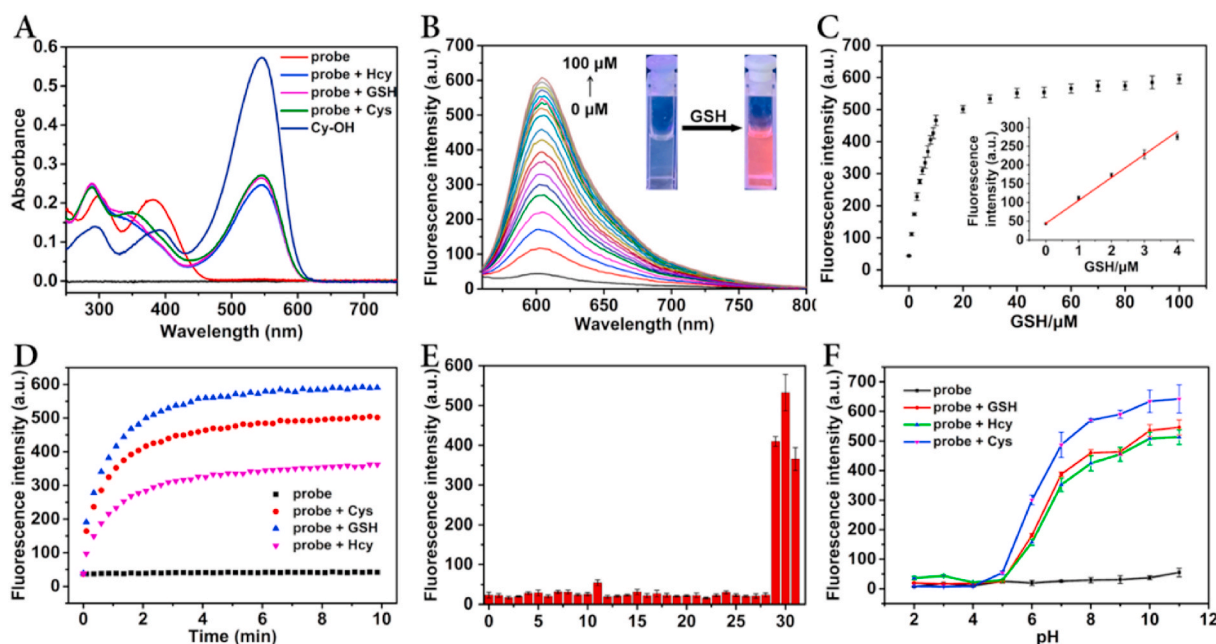


Fig. 1. Photophysical properties of **Cy-DNBS**. (A) Absorption spectra of **Cy-DNBS** (10 μM) and **Cy-OH** (10 μM) in phosphate buffered saline (PBS, 0.01 mM, pH 7.4 containing 10% DMSO) before and after addition of thiols (100 μM). (B) Fluorescence spectra changes of **Cy-DNBS** (10 μM) upon addition of different concentrations of GSH in phosphate buffered saline (PBS, 0.01 mM, pH 7.4 containing 10% DMSO). (C) Fluorescence intensity at 604 nm as a function of GSH concentration. Insert: Linear relationship of fluorescence intensity at 604 nm as a function of GSH concentration, $y = 52.758 + 55.524[\text{GSH}]$, with $R^2 = 0.9932$. (D) Changes in fluorescence intensity at 604 nm in the absence and presence of GSH, Cys and Hcy (100 μM) as a function of reaction time, respectively. (E) Fluorescence responses of **Cy-DNBS** (10 μM) to various biological species. 0–31: blank, Na^+ (1 mM), Cl^- (1 mM), HCO_3^- (1 mM), CH_3COO^- (1 mM), NO_2^- (1 mM), HPO_4^{2-} (1 mM), H_2PO_4^- (1 mM), CO_3^{2-} (1 mM), Ca^{2+} (1 mM), SO_3^{2-} (1 mM), $\text{S}_2\text{O}_3^{2-}$ (1 mM), HSO_4^- (1 mM), Pro (100 μM), Tyr (100 μM), Met (100 μM), His (100 μM), Trp (100 μM), Ile (100 μM), Gly (100 μM), Asn (100 μM), Ala (100 μM), Val (100 μM), Thr (100 μM), Ser (100 μM), Arg (100 μM), Phe (100 μM), Leu (100 μM), Lys (100 μM), GSH (100 μM), Cys (100 μM), Hcy (100 μM). (F) Fluorescence intensity changes of **Cy-DNBS** (10 μM) at 604 nm before and after addition of GSH, Cys and Hcy (100 μM) in phosphate buffered saline at different pH.

Furthermore, we tested time-dependent fluorescence spectra of **Cy-DNBS** with GSH, Cys and Hcy in phosphate buffered saline (PBS, 0.01 mM, pH 7.4 containing 10% DMSO). As illustrated in Fig. 1D and Fig. S4, the fluorescence intensity displays a time-dependent enhancement upon addition of 10 eq. GSH/Cys/Hcy. Within the first 2 min, the fluorescence intensity enhanced obviously and it took about 8 min to reach equilibrium. This indicated that the probe was capable to rapidly respond to thiols.

3.3. Selectivity

Selectivity is another crucial parameter of fluorescence probe[12]. To evaluate the selectivity of **Cy-DNBS** towards biothiols, we tested the response of **Cy-DNBS** to different biological species, including various amino acids and essential ions. Fig. 1E and Fig. S5 show the fluorescence intensity of **Cy-DNBS** towards the tested species. Upon the addition of GSH, Cys and Hcy, the fluorescence intensity of **Cy-DNBS** obviously enhanced. However, the emission exhibits a negligible change in the presence of other species. The UV–Vis spectra and color change of **Cy-DNBS** after addition of various species were shown in Fig. S6–S7, respectively. All these results demonstrated that **Cy-DNBS** has excellent selectivity towards thiols.

3.4. Effect of pH on response performance

It was found that the pH value of solution was crucial to the cleavage reaction[37]. To explore the effect of pH on our probe, we examined the fluorescence responses of 10 μM **Cy-DNBS** at 604 nm in the absence and presence of 100 μM thiols at different pH. Fig. 1F showed that the probe itself was stable and underwent negligible change in emission from pH 2.0 to 11.0. Upon the addition of thiols, no fluorescence enhancement

could be observed in pH range of 2.0–5.0. However, in pH range of 5.0–11.0, the fluorescence signal was obviously increased. All these demonstrated that **Cy-DNBS** was suitable for use under physiological conditions.

3.5. Cytotoxicity assay

Before the application of probe **Cy-DNBS** in fluorescent imaging in living cells, the cellular cytotoxicity of **Cy-DNBS** to HeLa cells was

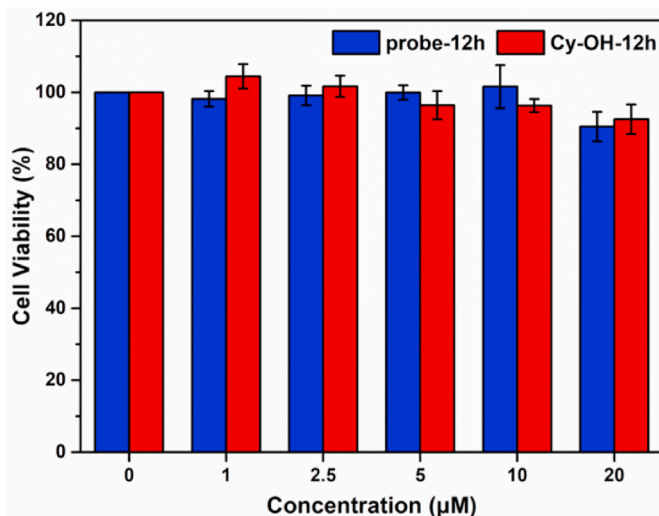


Fig. 2. Cell viability values (%) of HeLa cells estimated by cell counting kit-8 (CCK-8) assay. HeLa cells were cultured with **Cy-DNBS** and **Cy-OH** for 12 h.

estimated using the standard cell counting kit-8 (CCK-8) assay. As shown in Fig. 2, after cultured with different concentrations (0–20 μM) of **Cy-DNBS** and **Cy-OH** for 12 h, more than 80% of cells remained alive, the results exhibited the low cytotoxicity of **Cy-DNBS**. The CCK-8 assays were also conducted in other cells, including Du 145, PC-12 and HUVEC cells (Fig. S8).

3.6. Cell imaging

Since the indole ammonium moiety of **Cy-DNBS** owns a positive charge, it tends to accumulate in mitochondria through electrostatic interactions due to the mitochondrial membrane negative potential[11]. To confirm the subcellular distribution of **Cy-DNBS**, fluorescence co-localization experiments were conducted using MitoTracker® Green FM, a commercially available mitochondrial specific fluorescent dye. As illustrated in Fig. 3, the fluorescence of **Cy-DNBS** in red channel responding to thiols overlaps perfectly with that of the MitoTracker® Green FM, with a high Pearson's correlation coefficient of 0.91. In contrast, the fluorescence of probe in red channel overlaps poorly with that of Hoechst 33342, a commercial blue-fluorescent nucleus dye, with a low Pearson's correlation coefficient of 0.26. In addition, to further confirm the mitochondrial targeting ability of the probe, co-localization experiments were also conducted in other cancer cells, including Du 145 (Human prostate cancer cell) and PC-12 cells (rat adrenal chromaffin cells) (Fig. S9–S10). Finally, all results are similar with those of HeLa. These results strongly indicate that **Cy-DNBS** has excellent ability to target mitochondria in living cells.

Inspired by the above advantages, we further validated the ability of **Cy-DNBS** for imaging endogenous thiols in living HeLa cells. As shown in Fig. 4, the HeLa cells alone showed no fluorescence. After cultured with **Cy-DNBS** (5 μM) at 37 °C for 30 min, the cells displayed distinct red fluorescence, owing to the formation of **Cy-OH**. The results indicated that **Cy-DNBS** could efficiently permeate into cells and react with the thiols to produce fluorescence. However, when the cells were pre-treated with 500 μM N-phenylmaleimide (NMM, a well-known thiol scavenger) for 30 min, followed by incubation with **Cy-DNBS** (5 μM) for 30 min, quite weak fluorescence was observed, indicating the

fluorogenic performance of **Cy-DNBS** is indeed attributed to the thiol interaction. To show the versatile live cell-imaging application of **Cy-DNBS**, fluorescence imaging experiments were also conducted in living Du 145 and PC-12 cells (Fig. S11–S12), both of which exhibited similar results as HeLa. These results confirmed that **Cy-DNBS** can be used as a powerful tool for bioimaging in various cancer cells.

Many evidences suggest that mitochondria maintain the cellular redox homeostasis and the intracellular thiol levels are related to mitochondria oxidative stress[13]. In order to evaluate whether the probe **Cy-DNBS** can detect the fluctuations in thiol levels caused by oxidative stress in living cells, we first evaluated the effect of H_2O_2 on responses of **Cy-DNBS** toward thiols in vitro (Fig. S13). We then employed **Cy-DNBS** to image thiols in living HeLa cells stimulated with H_2O_2 . As shown in Fig. 5, compared with those untreated with H_2O_2 , HeLa cells pre-treated with H_2O_2 (1 mM) for 30 min displayed a distinct decrease reduced fluorescence emission. These results suggested that the reduced thiols concentration is caused by H_2O_2 consumption or oxidation. Thus, **Cy-DNBS** can be used as a powerful probe for monitoring intracellular thiols fluctuation induced by oxidative stress.

4. Conclusions

In summary, we successfully designed and synthesized a cyanine-based, mitochondria-targetable fluorescent off-on probe, **Cy-DNBS**, for thiols imaging. The probe used indole ammonium moiety as the mitochondrial target site and DNBS group as the fluorescence quencher as well as the recognition site. This probe rapidly and selectively responded to thiols with high sensitivity over other related biological species. In addition, **Cy-DNBS** demonstrated low cytotoxicity and great membrane permeability to living cells, which allowed it to be successfully applied in bioimaging. Most importantly, the probe was able to image endogenous thiols and efficiently target mitochondria to evaluate mitochondrial oxidative stress level induced by H_2O_2 . Consequently, the probe has a potential to serve as a powerful tool for monitoring cellular thiols and providing insight into biological behavior.

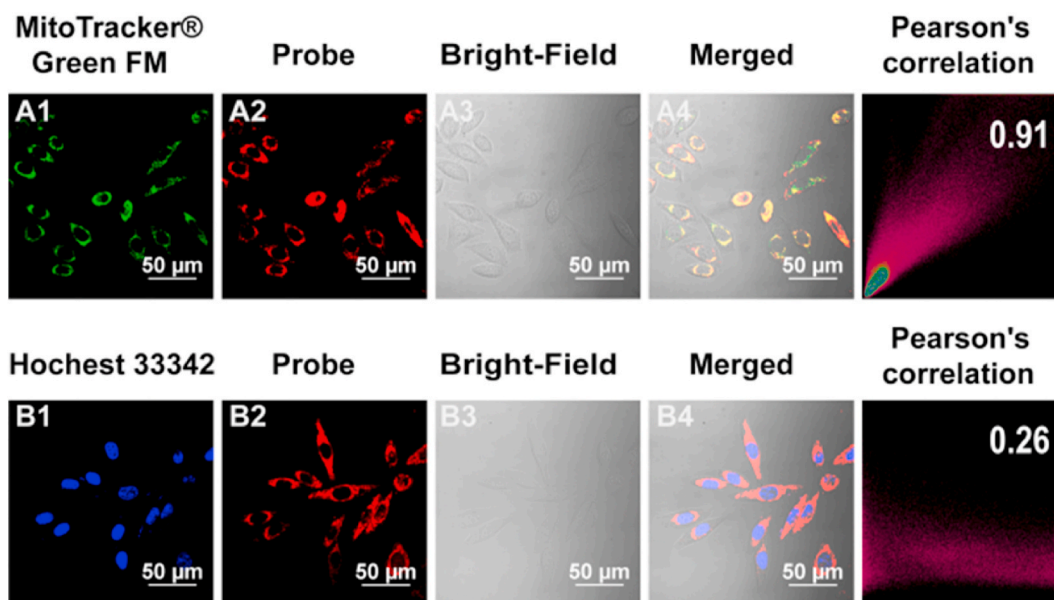


Fig. 3. Colocalization imaging of living HeLa cells. (A) The cells were cultured with MitoTracker® Green FM (250 nM) for 30 min and then cultured with 5 μM **Cy-DNBS** for 30 min. (B) The cells were cultured with Hoechst 33342 (5 $\mu\text{g}/\text{mL}$) for 30 min and then cultured with 5 μM **Cy-DNBS** for 30 min. (A1) Emission from MitoTracker® Green FM channel, $\lambda_{\text{ex}} = 488 \text{ nm}$, $\lambda_{\text{em}} = 500\text{--}550 \text{ nm}$. (B1) Emission from Hoechst 33342 channel, $\lambda_{\text{ex}} = 404 \text{ nm}$, $\lambda_{\text{em}} = 425\text{--}475 \text{ nm}$. (A2, B2) Emission from **Cy-DNBS** channel, $\lambda_{\text{ex}} = 561 \text{ nm}$, $\lambda_{\text{em}} = 570\text{--}620 \text{ nm}$. (A3, B3) Bright-Field image. (A4, B4) Merged image of A1–A3, B1–B3, respectively. (A5, B5) Colocalization coefficient (Pearson's coefficient) of (A1) and (A2), (B1) and (B2), respectively. Scale bar: 50 μm .

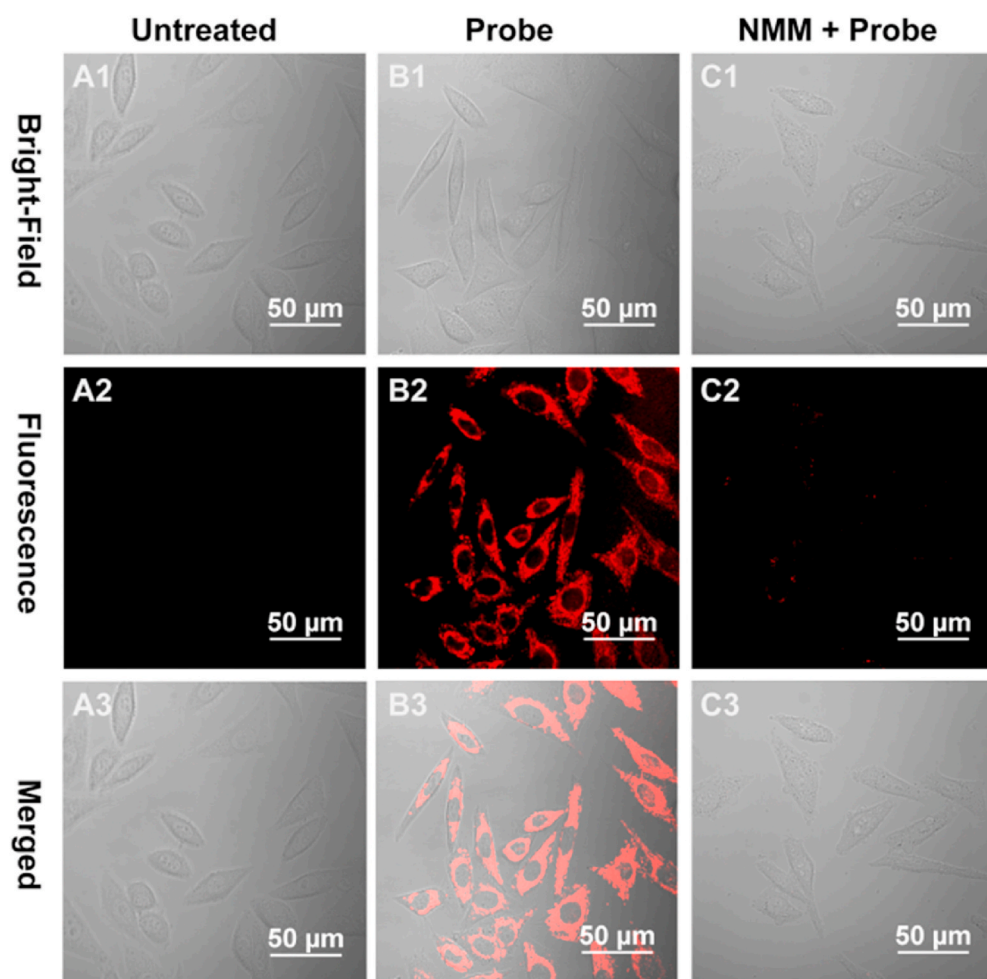


Fig. 4. Confocal fluorescence images of Cy-DNBS responding to endogenous biothiols in living HeLa cells. (A) Fluorescence image of HeLa cells; (B) Fluorescence image of HeLa cells cultured with Cy-DNBS (5 μM) at 37 °C for 30 min; (C) Fluorescence image of HeLa cells pre-treated with N-methylmaleimide (NMM, 500 μM) for 30 min followed by incubation with Cy-DNBS (5 μM) at 37 °C for 30 min. First row: bright-field image; second row: red channel of 570–620 nm ($\lambda_{ex} = 561$ nm); third row: merged bright field images with red channel images. Scale bar: 50 μm.

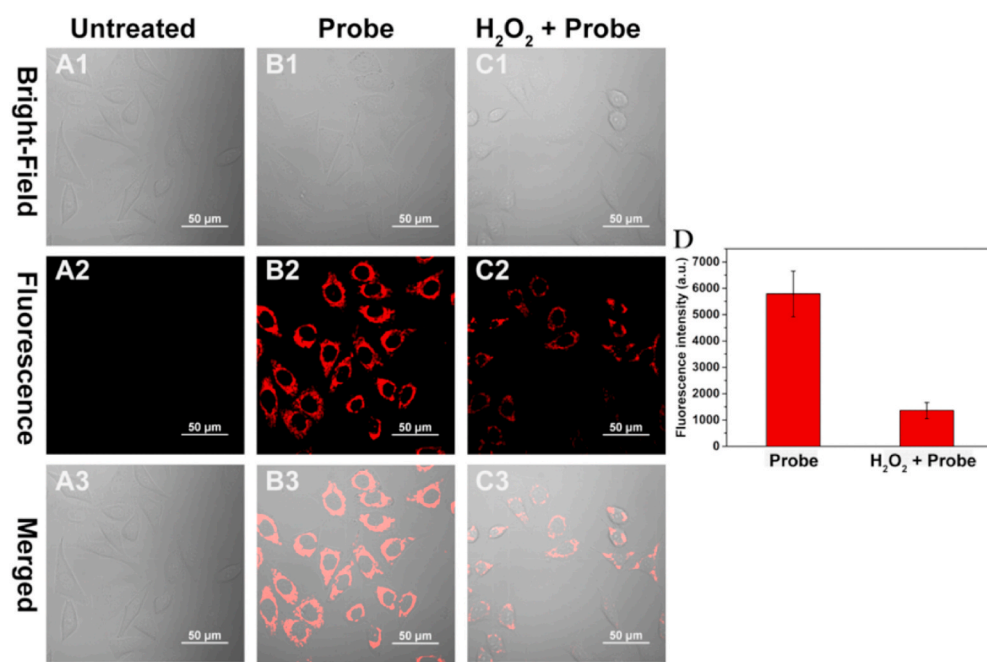


Fig. 5. Confocal fluorescence images of Cy-DNBS in living HeLa cells. (A) Fluorescence image of HeLa cells; (B) Fluorescence image of HeLa cells cultured with Cy-DNBS (5 μM) at 37 °C for 30 min; (C) Fluorescence image of HeLa cells pre-treated with H₂O₂ (1 mM) for 30 min followed by incubation with Cy-DNBS (5 μM) at 37 °C for 30 min. First row: bright-field image; second row: red channel of 570–620 nm ($\lambda_{ex} = 561$ nm); third row: merged bright field images with red channel images. (D) The quantification of fluorescence intensity of the (B) and (C) group. Scale bar: 50 μm.

CRedit authorship contribution statement

Yuedong Zhu: Investigation, Synthesis, Spectral testing and cell imaging, Data curation, Writing – original draft. **Haiting Pan:** Spectral testing and cell imaging. **Yanyan Song:** Cell imaging. **Chao Jing:** Writing – review & editing. **Jia-An Gan:** Writing – review & editing. **Junji Zhang:** Conceptualization, Resources, Supervision, Writing – review & editing.

Declaration of competing interest

The authors declare that they have no known competing financial interests or personal relationships that could have appeared to influence the work reported in this paper.

Acknowledgments

The project was supported by NSFC (21878086), the Shanghai Rising-Star Program (19QA1402500 to J. Z.), Shanghai Sailing Program (18YF1405700 to C. J.) and the Fundamental Research Funds for the Central Universities (222201717003). The authors acknowledge also acknowledge the Shanghai Municipal Science and Technology Major Project (Grant No.2018SHZDZX03) and the international cooperation program of Shanghai Science and Technology Committee (17520750100).

Appendix A. Supplementary data

Supplementary data to this article can be found online at <https://doi.org/10.1016/j.dyepig.2021.109376>.

References

- Han CM, Yang HR, Chen M, Su QQ, Feng W, Li FY. Mitochondria-targeted near-infrared fluorescent off-on probe for selective detection of cysteine in living cells and in vivo. *ACS Appl Mater Interfaces* 2015;7(50):27968–75. <https://doi.org/10.1021/acsami.5b10607>.
- Xu W, Teoh CL, Peng JJ, Su DD, Yuan L, Chang YT. A mitochondria-targeted ratiometric fluorescent probe to monitor endogenously generated sulfur dioxide derivatives in living cells. *Biomaterials* 2015;56:1–9. <https://doi.org/10.1016/j.biomaterials.2015.03.038>.
- Zhou J, Li LH, Shi W, Gao XH, Li XH, Ma HM. HOCl can appear in the mitochondria of macrophages during bacterial infection as revealed by a sensitive mitochondrial-targeting fluorescent probe. *Chem Sci* 2015;6(8):4884–8. <https://doi.org/10.1039/c5sc01562f>.
- Shu W, Wu YL, Zang SP, Su S, Kang H, Jing J, Zhang XL. A mitochondria-targeting highly specific fluorescent probe for fast sensing of endogenous peroxynitrite in living cells. *Sensor Actuator B Chem* 2020;303:127284. <https://doi.org/10.1016/j.snb.2019.127284>.
- Li XY, Fang P, Mai JT, Choi ET, Wang H, Yang XF. Targeting mitochondrial reactive oxygen species as novel therapy for inflammatory diseases and cancers. *J Hematol Oncol* 2013;6. <https://doi.org/10.1186/1756-8722-6-19>.
- Li P, Zhang W, Li KX, Liu X, Xiao HB, Zhang W, Tang B. Mitochondria-targeted reaction-based two-photon fluorescent probe for imaging of superoxide anion in live cells and in vivo. *Anal Chem* 2013;85(20):9877–81. <https://doi.org/10.1021/ac402409m>.
- Zang SP, Shu W, Shen TJ, Gao CC, Tian Y, Jing J, Zhang XL. Palladium-triggered ratiometric probe reveals CO's cytoprotective effects in mitochondria. *Dyes Pigments* 2020;173:107861. <https://doi.org/10.1016/j.dyepig.2019.107861>.
- Shu W, Wu YL, Shen TJ, Cui J, Kang H, Jing J, Zhang XL. A mitochondria-targeted far red fluorescent probe for ratiometric imaging of endogenous peroxynitrite. *Dyes Pigments* 2019;170:107609. <https://doi.org/10.1016/j.dyepig.2019.107609>.
- Huang YF, Zhang YB, Huo FJ, Chao JB, Cheng FQ, Yin CX. A new strategy: distinguishable multi-substance detection, multiple pathway tracing based on a new site constructed by the reaction process and its tumor targeting. *J Am Chem Soc* 2020;142(43):18706–14. <https://doi.org/10.1021/jacs.0c10210>.
- Liu ZK, Wang QQ, Wang H, Su WT, Dong SL. A FRET based two-photon fluorescent probe for visualizing mitochondrial thiols of living cells and tissues. *Sensors* 2020;20(6). <https://doi.org/10.3390/s20061746>.
- Yang YT, Zhou TT, Jin M, Zhou KY, Liu DD, Li X, Huo FJ, Li W, Yin CX. Thiol-chromene "click" reaction triggered self-immolative for MR visualization of thiol flux in physiology and pathology of living cells and mice. *J Am Chem Soc* 2019;142(3):1614–20. <https://doi.org/10.1021/jacs.9b12629>.
- Chen ZY, Sun Q, Yao YH, Fan XX, Zhang WB, Qian JH. Highly sensitive detection of cysteine over glutathione and homo-cysteine: new insight into the Michael addition of mercapto group to maleimide. *Biosens Bioelectron* 2017;91:553–9. <https://doi.org/10.1016/j.bios.2017.01.013>.
- Yin J, Kwon Y, Kim D, Lee D, Kim G, Hu Y, Ryu JH, Yoon J. Cyanine-based fluorescent probe for highly selective detection of glutathione in cell cultures and live mouse tissues. *J Am Chem Soc* 2014;136(14):5351–8. <https://doi.org/10.1021/ja412628z>.
- Li P, Shi XH, Xiao HB, Ding Q, Bai XY, Wu CC, Zhang W, Tang B. Two-photon imaging of the endoplasmic reticulum thiol flux in the brains of mice with depression phenotypes. *Analyst* 2019;144(1):191–6. <https://doi.org/10.1039/c8an01626g>.
- Yu FB, Li P, Wang BS, Han KL. Reversible near-infrared fluorescent probe introducing tellurium to mimetic glutathione peroxidase for monitoring the redox cycles between peroxynitrite and glutathione in vivo. *J Am Chem Soc* 2013;135(20):7674–80. <https://doi.org/10.1021/ja401360a>.
- Yang XP, Liu WY, Tang J, Li P, Weng HB, Ye Y, Xian M, Tang B, Zhao YF. A multi-signal mitochondria-targeted fluorescent probe for real-time visualization of cysteine metabolism in living cells and animals. *Chem Commun* 2018;54(81):11387–90. <https://doi.org/10.1039/c8cc05418e>.
- Lim CS, Masanta G, Kim HJ, Han JH, Kim HM, Cho BR. Ratiometric detection of mitochondrial thiols with a two-photon fluorescent probe. *J Am Chem Soc* 2011;133(29):11132–5. <https://doi.org/10.1021/ja205081s>.
- Chen XQ, Zhou Y, Peng XJ, Yoon J. Fluorescent and colorimetric probes for detection of thiols. *Chem Soc Rev* 2010;39(6):2120–35. <https://doi.org/10.1039/b925092a>.
- Yin CX, Huo FJ, Zhang JJ, Martinez-Manez R, Yang YT, Lv HG, Li SD. Thiol-addition reactions and their applications in thiol recognition. *Chem Soc Rev* 2013;42(14):6032–59. <https://doi.org/10.1039/c3cs60055f>.
- Yue YK, Huo FJ, Ning P, Zhang YB, Chao JB, Meng XM, Yin CX. Dual-site fluorescent probe for visualizing the metabolism of Cys in living cells. *J Am Chem Soc* 2017;139(8):3181–5. <https://doi.org/10.1021/jacs.6b12845>.
- Qiao D, Shen TL, Zhu MY, Liang X, Zhang L, Yin Z, Wang BH, Shang LQ. A highly selective and sensitive fluorescent probe for simultaneously distinguishing and sequentially detecting H₂S and various thiol species in solution and in live cells. *Chem Commun* 2018;54(94):13252–5. <https://doi.org/10.1039/c8cc07761d>.
- Lee HY, Choi YP, Kim S, Yoon T, Guo ZQ, Lee S, Swamy KMK, Kim G, Lee JY, Shin I, Yoon J. Selective homocysteine turn-on fluorescent probes and their bioimaging applications. *Chem Commun* 2014;50(53):6967–9. <https://doi.org/10.1039/c4cc00243a>.
- Hwang C, Sinskey AJ, Lodish HF. Oxidized redox state of glutathione in the endoplasmic reticulum. *Science* 1992;257(5076):1496–502. <https://doi.org/10.1126/science.1523409>.
- Liu B, Wang JF, Zhang G, Bai RK, Pang Y. Flavone-based ESIPT ratiometric chemodosimeter for detection of cysteine in living cells. *ACS Appl Mater Interfaces* 2014;6(6):4402–7. <https://doi.org/10.1021/am500102s>.
- Zhou JL, Xu S, Dong XC, Zhao WL, Zhu QG. 3,5-dinitropropyridin-2-yl as a fast thiol-responsive capping moiety in the development of fluorescent probes of biothiols. *Dyes Pigments* 2019;167:157–63. <https://doi.org/10.1016/j.dyepig.2019.04.020>.
- Fu ZH, Han X, Shao YL, Fang JG, Zhang ZH, Wang YW, Peng Y. Fluorescein-based chromogenic and ratiometric fluorescence probe for highly selective detection of cysteine and its application in bioimaging. *Anal Chem* 2017;89(3):1937–44. <https://doi.org/10.1021/acs.analchem.6b04431>.
- Fan JL, Han ZC, Kang Y, Peng XJ. A two-photon fluorescent probe for lysosomal thiols in live cells and tissues. *Sci Rep* 2016;6:2045–322. <https://doi.org/10.1038/srep19562>.
- Xu ZQ, Huang XT, Han X, Wu D, Zhang BB, Tan Y, Cao MJ, Liu SH, Yin J, Yoon JY. A visible and near-infrared, dual-channel fluorescence-on probe for selectively tracking mitochondrial glutathione. *Inside Chem* 2018;4(7):1609–28. <https://doi.org/10.1016/j.chempr.2018.04.003>.
- Yin CX, Xiong KM, Huo FJ, Salamaña JC, Strongin RM. Fluorescent probes with multiple binding sites for the discrimination of Cys, hcy, and GSH. *Angew Chem Int Ed* 2017;56(43):13188–98. <https://doi.org/10.1002/anie.201704084>.
- Liu ZX, Zhou X, Miao Y, Hu Y, Kwon N, Wu X, Yoon J. A reversible fluorescent probe for real-time quantitative monitoring of cellular glutathione. *Angew Chem Int Ed* 2017;56(21):5812–6. <https://doi.org/10.1002/anie.201702114>.
- Yang YZ, Xu ZY, Han L, Fan YZ, Qing M, Li NB, Luo HQ. A simple fluorescent probe with two different fluorescence signals for rapid sequence distinguishing of Cys/Hcy/GSH and intracellular imaging. *Dyes Pigments* 2021;184. <https://doi.org/10.1016/j.dyepig.2020.108722>.
- Tong HJ, Zhao JH, Li XM, Zhang YJ, Ma SN, Lou KY, Wang W. Orchestration of dual cyclization processes and dual quenching mechanisms for enhanced selectivity and drastic fluorescence turn-on detection of cysteine. *Chem Commun* 2017;53(25):3583–6. <https://doi.org/10.1039/c6cc09336a>.
- Kand D, Kalle AM, Varma SJ, Talukdar P. A chromenoquinoline-based fluorescent off-on thiol probe for bioimaging. *Chem Commun* 2012;48(21):2722–4. <https://doi.org/10.1039/c2cc16593g>.
- Xu Z, Xu L. Fluorescent probes for the selective detection of chemical species inside mitochondria. *Chem Commun* 2016;52(6):1094–119. <https://doi.org/10.1039/c5cc09248e>.
- Zhang PS, Wang H, Hong YX, Yu ML, Zeng RJ, Long YF, Chen J. Selective visualization of endogenous hypochlorous acid in zebrafish during lipopolysaccharide-induced acute liver injury using a polymer micelles-based ratiometric fluorescent probe. *Biosens Bioelectron* 2018;99:318–24. <https://doi.org/10.1016/j.bios.2017.08.001>.
- Wang H, Zhang PS, Tian Y, Zhang Y, Yang HP, Chen S, Zeng RJ, Long YF, Chen J. Real-time monitoring of endogenous cysteine levels in living cells using a CD-based

- ratiometric fluorescent nanoprobe. *Anal Bioanal Chem* 2018;410(18):4379–86. <https://doi.org/10.1007/s00216-018-1091-x>.
- [37] Peng L, Zhou ZJ, Wei RR, Li K, Song PS, Tong AJ. A fluorescent probe for thiols based on aggregation-induced emission and its application in live-cell imaging. *Dyes Pigments* 2014;108:24–31. <https://doi.org/10.1016/j.dyepig.2014.04.020>.
- [38] Mao YY, Du HH, Wang XC, Tian M, Wang Y, Liu L, Wei JM, Xue FF, Liu GD, Zhang XJ, Yi T. A ratiometric fluorescent probe for rapidly detecting bio-thiols in vitro and in living cells. *Dyes Pigments* 2019;171. <https://doi.org/10.1016/j.dyepig.2019.107688>.
- [39] Maeda H, Matsuno H, Ushida M, Katayama K, Saeki K, Itoh N. 2,4-dinitrobenzenesulfonyl fluoresceins as fluorescent alternatives to Ellman's reagent in thiol-quantification enzyme assays. *Angew Chem Int Ed* 2005;44(19):2922–5. <https://doi.org/10.1002/anie.200500114>.